FEATURE CURVE-GUIDED VOLUME RECONSTRUCTION FROM 2D IMAGES

Yunhao Tan, Jing Hua, Ming Dong

Department of Computer Science
Wayne State University, Detroit, MI 48202

ABSTRACT

In this paper, we propose a new paradigm to reconstruct 3D volume from histology slices guided by NURBS spline-based feature curves. Histology slices are first scanned into computer as a sequence of image files with a histology film scanner. An initial 3D alignment of the images is obtained through the histological similarity matching between neighboring slices. Further optimization is achieved by applying optimal affine transformation to each slice according to feature curve smoothing. Considering the intrinsic smoothness of the physical features, we compute the transformation to refine the selected features based on NURBS splines. Consequently, volume reconstruction is further optimized. We also present new evaluation methods to prove that our reconstruction scheme can achieve a high accuracy.

Index Terms— Feature Curve, Volume Reconstruction.

1. INTRODUCTION

Histology is the study of tissue sectioned as a thin slice, using a microtome. It is an important tool in biology and medical domain. Although informative itself, histology provides little information of the overall 3D biological structures and physical attributes. Naturally 3D histology technique becomes more and more important in histology analysis and visualization. If each slice image is properly transformed and arranged in a sequential order, one discretized structured-grid volume can be obtained. This procedure is also called registration or alignment. The biggest challenge in the procedure is to achieve a "proper" transformation which can minimize the registration error.

In order to establish such a highly desirable 3D histology technique, lots of research efforts from both academia and industry have been devoted to this research topic. Chan *et al.* proposed a methodology for making optimal registration decisions during 3D volume reconstruction [1]. Lee *et al.* presented a fusion-based approach to address the problem of 3D volume reconstruction from depth adjacent sub-volumes acquired using a confocal laser scanning microscope(CLSM) [2]. Readers may find other relevant literature in [3, 4, 5, 6].

Thanks to MTTC for funding.

It's both intuitive and mathematically proved that inserted fiducial agents can dramatically reduce registration error by being used as references during the reconstruction. Currently, the most common, widely adopted method in this domain is to insert several parallel appendices into the embed wax. Methodologists usually choose materials sustainable to the further processes such as sectioning, washing and dyeing. However, this manual and laborious procedure inevitably causes extra time and expense. Moreover, this method does not apply to existing histology data which have already been prepared without fiducial marks. Besides viable 3D histology techniques, another urgent need is the effective evaluation methods for assessing the accuracy and quality of the 3D reconstruction of histology images.

To alleviate the aforementioned difficulties, we make use of the intrinsic features inherited in the sequence of histology slices and model the features with NURBS curves. Based on these NURBS-based feature curves, a new paradigm to reconstruct 3D histology volume is presented in this paper. An initial 3D alignment of the images is first obtained through the histological similarity matching between neighboring slices. Further optimization is achieved by applying optimal affine transformation to each slice according to NURBS-based feature curve smoothing. Consequently, volume reconstruction is further optimized. We also present two new evaluation methods to prove that our reconstruction scheme can achieve a high accuracy. These two evaluation methods can be generally used in evaluation of 3D histology data reconstruction.

This paper is organized in the following way. Section 2 introduces the initial alignment by fusing the inner physical features of histology. Section 3 proposes a novel method which uses NURBS spline to retrieve the optimal transformation that can be applied to refine the volume. Experiments and results will be presented in Section 4 followed by a summary in Section 5.

2. INITIAL ALIGNMENT OF 2D SLICES

Before the structure of 3D histology can be explored and analyzed, generating a high-fidelity 3D volume is a crucial and preliminary step in which all histology slices need to be stacked into one volume. Structured-grid volume representation can be employed here and we choose Analyze 7.5 file format

which is already a well-established industry standard.

2.1. Digital Scan of 2D Histology Slices

At first 2D histology slices are scanned into computer through a digital histology film scanner. This device can differentiate the level-of-detail of cell structure of the histology and produce high-quality images. In this step, necessary image processing filters, for instance, Gaussian smoother, will be applied to the raw data due to the inevitable noises. Figure 1(a) and Figure 1(b) are two original scanned images from two histology data slices.

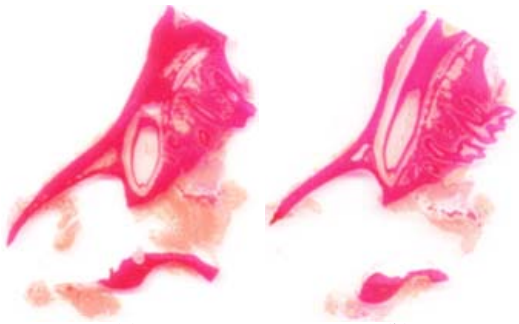

(a) (b)

Fig. 1. (a) An original image scanned from one histology data slice; (b) Image of anther slice which is not a consecutive from the previous one. Histology structures of these two slices are different.

2.2. Initial Alignment through Similarity Matching

The similarity matching of adjacent slices is based on a biological fact: in each two neighboring histology data slices there is no high-order discontinuity in the histology structure, i.e., there exists certain histology similarity which can be used to match adjacent slices. Based on this observation, we need to minimize the following equation:

$$\min DIFF_{den} = \sum_{i=1}^{n-1} \|I(i) - T \cdot I(i+1)\|^2 \qquad (1)$$

where $I(i)$ indicates the density distribution of i^{th} slice. $I(i+1)$ is subject to the affine transformation matrix T. Here we select the i^{th} slice as the stationary one, and apply affine transformation to the $(i+1)^{th}$ slice. The correspondent affine transformation T is a 4×4 matrix as below:

$$\begin{bmatrix} x' \\ y' \\ z' \\ 1 \end{bmatrix} = T \begin{bmatrix} x \\ y \\ z \\ 1 \end{bmatrix} \qquad (2)$$

where $T = \begin{bmatrix} t_{00} & t_{01} & t_{02} & t_{03} \\ t_{10} & t_{11} & t_{12} & t_{13} \\ t_{20} & t_{21} & t_{22} & t_{23} \\ t_{30} & t_{31} & t_{32} & t_{33} \end{bmatrix}$, and $\begin{bmatrix} x \\ y \\ z \\ 1 \end{bmatrix}$ denotes the original position of a voxel and $\begin{bmatrix} x' \\ y' \\ z' \\ 1 \end{bmatrix}$ denotes the transformed position. Because we use homogeneous coordinates here, the position vector in equation 2 is extended to order 4. Here T is the combination of rotation factor and translation factor. Equation (1) is essentially a least square problem. Solving this system, we can obtain a set of transformations which construct an initial alignment of all 2D histology data slices.

3. REFINEMENT THROUGH THE NURBS-BASED FEATURE CURVE FAIRING

The quality of the volume reconstruction can be further improved through further refinement. Here we proposed a new method based on the same fact that structural feature curves in histology data are smooth. Considering that Non-Uniform Rational B-Spline (NURBS) is an ideal mathematic representation to model natural objects and phenomena, we use NURBS to perform the further refinement. The fundamental idea here is to streamline the features of the histology to make the entire volume registered better.

3.1. NURBS Curve

In descriptive geometry domain, NURBS has been widely accepted because its insurmountable merits: affine invariance, convex hull, clear geometric interpretation, and so on.

A NURBS[7] is a vector-valued piecewise rational polynomial function of the form:

$$C(u) = \frac{\sum_{i=0}^{n} w_i P_i N_{i,p}(u)}{\sum_{i=0}^{n} w_i N_{i,p}(u)}, \qquad a \le u \le b \qquad (3)$$

where the w_i are non-negative scalar value called the weights, the P_i are the control points and the $N_{i,p}(u)$ are the p^{th} degree B-spline basis function defined recursively as

$$N_{i,p}(u) = \frac{u - u_i}{u_{i+p} - u_i} N_{i,p-1}(u) + \frac{u_{i+p+1} - u}{u_{i+p+1} - u_{i+1}} N_{i+1,p-1}(u) \qquad (4)$$

$$N_{i,0}(u) = \begin{cases} 1 & \text{if } u_i \le u \le u_{i+1} \\ 0 & \text{otherwise} \end{cases} \qquad (5)$$

where u_i are real numbers called knots which form a knot vector $U = u_0, \cdots, u_m$ with $u_i \le u_{i+1}$ for $i = 0, \cdots, m$.

The degree, p, number of knots, $m+1$, and number of control points, $n+1$, are confined by the formula $m = n + p + 1$. In order that the curve passes the first control point and the last one, i.e., P_0 and P_n, the end knots u_0 and u_m should

repeat with multiplicity $p+1$, i.e., $u_0 = u_1 =, \cdots, = u_p$ and $u_{m-p} = u_{m-p+1} =, \cdots, = u_m$. For more information about B-Splines, please refer to [8].

3.2. Identification of Feature Points

It would be time-consuming and laborious to identify the feature points manually considering the number of slices, although it is intuitive at first glance. Here we use a curvature-based approach. After tracking the contour of the tissue, we select three points which are the extremal of curvature as the features. Because the contour is a series of discrete vertices, we approximate the curvature using normalized edge vector difference of two neighboring vertices in the contour. Readers are referred to [9] for a complete description. Figure 2 shows the process concisely.

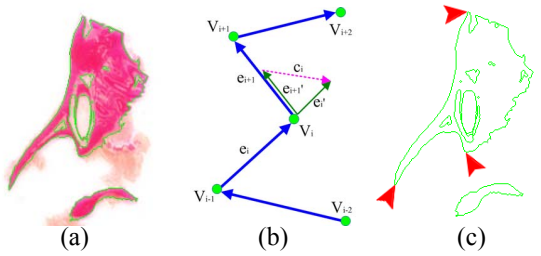

Fig. 2. (a) A histology slice and its contour retrieved shown in green; (b) A section of contour with 5 vertices. e_i and e_{i+1} are edge vectors, e'_i and e'_{i+1} are normalized edge vectors , and the curvature c_i is determined by the difference of e'_i and e'_{i+1}; (c) Feature points are selected from the sharpest curvatures of the contour and marked by the red arrows.

3.3. Creating NURBS Curve Using Feature Points

Suppose $p_0, p_1, ..., p_n$ are the $n+1$ feature points where p_0 comes from slice 0, p_1 comes from slice 1, etc. We build a degree d NURBS curve with these $n+1$ control points. In practice, we usually choose cubic NURBS, which is degree of three. The corresponding number of knots is $n+5$. To retain the positions of the first point and the last one, we force the NURBS curve to clamp. That's to say, we make the curve go through the first and last point, and force it to tangent to the first line segment (the line segment connecting p_0 and p_1) and last one (the line segment connecting p_{n-1} and p_n).

3.4. Resampling the Feature Points

Now what we obtain is a smooth cubic NURBS curve which uses the feature points as its control points. The next task is to resample the feature points. For each control point, we keep its z-component and get its correspondent x and y component from the curve. Because NURBS does not provide an explicit way to compute this point, we use classic bisection method to obtain it. Figure 3 shows an example. In the figure the ellipses stand for the histology slice and P_i stand for the features points identified.

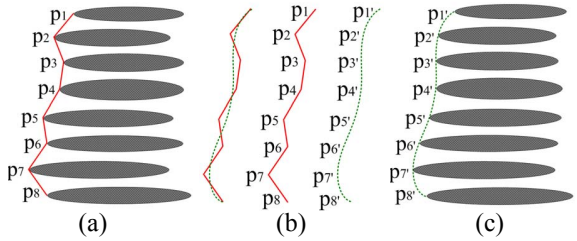

Fig. 3. (a) Initial alignment of eight slices with jig-jag appeared; (b) Line segments with control net, original positions, and new positions of feature points; (c) Realign the eight slices through further refinement.

3.5. Transformation based on Updated Feature Points

After we obtain the new locations of the feature points, we apply another round of affine transformation to each slice. The method here is the same as we use in Section 2.2. The difference is, in order to achieve the optimal affine transformation matrix, we need to only match selected points in each slice.

4. EXPERIMENTS AND RESULTS

To evaluate the registration and reconstruction quality, we proposed two novel methods: Comparison of all adjacent slices and Comparison between the reconstructed histology volume and the corresponding microCT(uCT) or MR imaging data.

In practice, uCT data may not be available. By showing the initial reconstructed volume, corresponding uCT volume, volume after refinement and corresponding uCT volume, Figure 4 demonstrates the feasibility of our paradigm qualitatively.

The first method is to compare all adjacent slices accumulatively. Mathematically the error is defined as:

$$err = \frac{\sum_{i=1}^{n-1} \|I(i) - I(i+1)\|}{\sum_{i=1}^{n-1} \|I(i)\|} \tag{6}$$

where $I(i)$ indicates the density distribution of i^{th} slice of the reconstructed volume. Table 1 shows the results of comparison of the samples.

The second one is to compare the reconstructed histology volume with the corresponding uCT volume. Because these two volumes are derived from two modalities, normalization and 3D co-registration should be applied to them at first, to make the comparison substantial. Then the error is defined by the rotation and translation factor between each pairing slices. To save the computational cost, here we compute the retrieved contour rather than the whole slice. Table 2 shows the results of comparison of one sample.

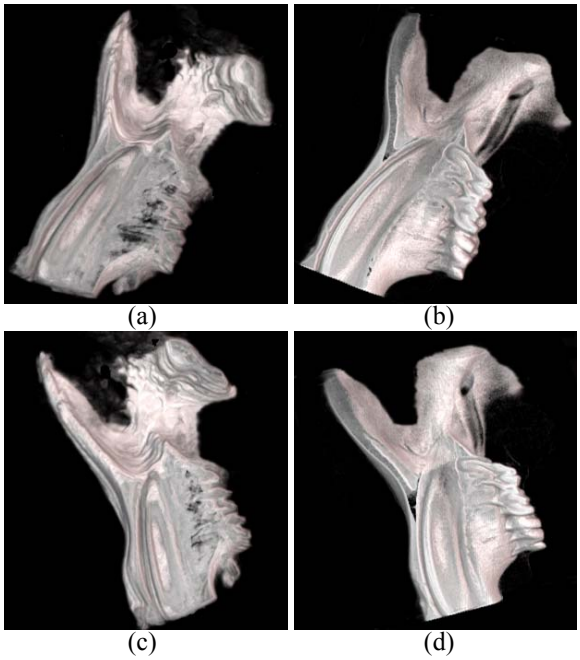

Fig. 4. (a) 3D visualization of reconstructed 3D histology volume after similarity mapping; (b) 3D visualization of the corresponding uCT volume from the same view point; (c) 3D visualization of reconstructed 3D histology volume after refinement; (d) 3D visualization of corresponding uCT volume from the same view point.

Sample ID	Pre-refinement	Post-refinement
1	2.851%	1.389%
2	3.045%	1.624%
3	3.199%	1.736%

Table 1. The experimental results of histology samples. Error is calculated as percentage.

5. CONCLUSION

We have presented a novel approach for 3D histology volume reconstruction from 2D histology slices or images. The contribution of this paper is that the paradigm we proposed is not only a fully automatic one (i.e., without human intervention), but also yields results at high accuracy. The initial alignment was gained through intrinsic biologic features similarity between neighboring slices, and further refinement was achieved by retrieving the optimal transformation through repositioning the feature points guided by NURBS modeling. The reconstructed 3D volume was evaluated by the comparison with corresponding uCT data. Quantitative results from experiments demonstrate the high accuracy of our framework.

Affine factor	Pre-refinement	Post-refinement
$Rotation$	1.981	0.957
$Translationt$	1.064	0.536

Table 2. The experimental results of histology samples. Unit for rotation is degree and unit for translation is pixel.

6. REFERENCES

[1] H. Chan and A. Chung, "Efficient 3d-3d vascular registration based on multiple orthogonal 2d projections," in *Second International Workshop on Biomedical Image Registration(WBIR 2003)*, 2003, vol. 2717, pp. 301–310.

[2] S. Lee and P. Bajcsy, "Three-dimensional volume reconstruction based on trajectory fusion from confocal laser scanning microscope images," in *Proceedings of IEEE Conference on Computer Vision and Pattern Recognition(CVPR 06)*, 2006, vol. 2, pp. 2221–2228.

[3] S. Choi, J. Lee, J. Kim, and M. Kim, "Volumetric object reconstruction using the 3d-mrf model-based segmentation," *IEEE Transctions on Medical Imaging*, vol. 16, no. 6, pp. 887–892, 1997.

[4] E. Bardinet, S. Ourselin, G. Malandain, D. Tande, K. Parain, N. Ayache, and J. Yelnik, "Three dimensional functional cartography of the human basal ganglia by registration of optical and histological serial sections," in *Proceedings of IEEE International Symposium on Biomedical Imaging*, 2002, pp. 329–332.

[5] R. Rosa, P. Chirco, and R. Massari, "Reconstruction corrections in advanced neutron tomography algorithms," *IEEE Transactions on Nuclear Science*, vol. 52, no. 1, pp. 400–403, 2005.

[6] S. Lee and P. Bajcsy, "Feature based registration of fluorescent lscm imagery using region centroids," in *Proceedings of SPIE International Symposium in Medical Imaging*, 2005, vol. 5747, pp. 170–181.

[7] L. Piegl, "On nurbs: A survey," in *IEEE Computer Graphcis and Applications*, 1991, vol. 11, pp. 55–71.

[8] G. Farin, *Curves and Surfaces for Computer-Aided Geometric Design*, Academic Press, 4 edition, 1996, Edited by Werner Rheinbolt.

[9] L. Amini, H. Soltanian-Zadeh, C. Lucas, and M. Gity, "Automatic segmentation of thalamus from brain mri integrating fuzzy clustering and dynamic contours," *IEEE Transactions on Biomedical Engineering*, vol. 51, no. 5, pp. 800–811, 2004.